SOLID PROPELLANT KINETICS. V. FUEL-OXIDIZER REACTION RATES FROM HETEROGENEOUS OPPOSED FLOW DIFFUSION FLAME

C. M. Ablow, et al

Stanford Research Institute

Prepared for:

Office of Naval Research
Defense Contract Administration Services Region

December 1974

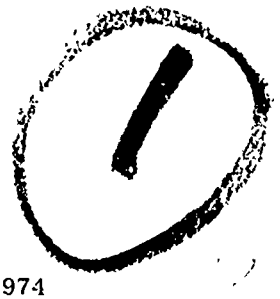

December 1974

SOLID PROPELLANT KINETICS

V. FUEL-OXIDIZER REACTION RATES FROM HETEROGENEOUS OPPOSED FLOW DIFFUSION FLAME*†

C. M. Ablow and H. Wise
Stanford Research Institute
Menlo Park, California 94025

† This work was sponsored by the Office of Naval Research, Power Branch, Washington, D.C., under Contract N00014-70-C-0155.

Unclassified

SECURITY CLASSIFICATION OF THIS PAGE (When Data Entered)

REPORT DOCUMENTATION PAGE

READ INSTRUCTIONS BEFORE COMPLETING FORM

1. REPORT NUMBER

2. GOVT ACCESSION NO.

3. RECIPIENT'S CATALOG NUMBER

4. TITLE (and Subtitle)

SOLID PROPELLANT KINETICS V. FUEL-OXIDIZER REACTION RATES FROM HETEROGENEOUS OPPOSED FLOW DIFFUSION FLAME

5. TYPE OF REPORT & PERIOD COVERED

Interim Report

6. PERFORMING ORG. REPORT NUMBER

PYU-8378

7. AUTHOR(s)

C. M. Ablow and H. Wise

8. CONTRACT OR GRANT NUMBER(s)

N00014-70-C-0155

9. PERFORMING ORGANIZATION NAME AND ADDRESS

Stanford Research Institute
Menlo Park, California 94025

10. PROGRAM ELEMENT, PROJECT, TASK AREA & WORK UNIT NUMBERS

NR-092-507

11. CONTROLLING OFFICE NAME AND ADDRESS

Office of Naval Research, Power Branch
Department of the Navy, Washington, D.C.

12. REPORT DATE

December 1974

13. NO. OF PAGES

37

15. SECURITY CLASS. (of this report)

Unclassified

14. MONITORING AGENCY NAME & ADDRESS (if diff. from Controlling Office)

DCASR - San Francisco
866 Malcolm Road
Burlingame, CA 94010

15a. DECLASSIFICATION/DOWNGRADING SCHEDULE

16. DISTRIBUTION STATEMENT (of this report)

Approved for public release;
Distribution of this document is unlimited.

DDC
RECEIVED
OCT 16 1975
D

17. DISTRIBUTION STATEMENT (of the abstract entered in Block 20, if different from report)

18. SUPPLEMENTARY NOTES

19. KEY WORDS (Continue on reverse side if necessary and identify by block number)

Diffusion Flame
Opposed Flow
Propellant Kinetics
Ammonium Perchlorate
Flame Model

20. ABSTRACT (Continue on reverse side if necessary and identify by block number)

A theoretical model is presented relating the gas dynamics and chemical kinetics of the opposed flow diffusion flame formed in the stagnation region between two opposing streams of gaseous reactants, one originating from the surface of a subliming solid, such as ammonium perchlorate. At low gas flows the regression rate of the solid is controlled by the physical properties of the system, including the net heat of gasification, the heat of combustion, and the transport parameters. At high gas flows a limiting solid regression rate is attained due to reaction-rate

DD FORM 1 JAN 73 1473

ON OF 1 NOV 65 IS OBSOLETE

Unclassified

SECURITY CLASSIFICATION OF THIS PAGE (When Data Entered)

SECURITY CLASSIFICATION OF THIS PAGE (When Data Entered)

19. KEY WORDS (Continued)

20 ABSTRACT (Continued)

limitations that cause incomplete combustion of the reactants. The theoretical model developed for the heterogeneous opposed flow diffusion flame allows interpretation of the limit in solid regression rates in terms of global reaction kinetics. Calculations have been carried out for a range of parameters, including net heats of gasification and activation energies. For the AP-propylene system the experimental data can be fitted to a second-order gas-phase reaction rate with an activation energy of 37 ± 1 kcal/mole and a preexponential coefficient of 10^{13} $cc \cdot mol^{-1} sec^{-1}$.

DD FORM 1 JAN 73 1473 (BACK)

EDITION OF 1 NOV 65 IS OBSOLETE

ABSTRACT

A theoretical model is presented relating the gas dynamics and chemical kinetics of the opposed flow diffusion flame formed in the stagnation region between two opposing streams of gaseous reactants, one originating from the surface of a subliming solid, such as ammonium perchlorate. At low gas flows the regression rate of the solid is controlled by the physical properties of the system, including the net heat of gasification, the heat of combustion, and the transport parameters. At high gas flows a limiting solid regression rate is attained due to reaction-rate limitations that cause incomplete combustion of the reactants. The theoretical model developed for the heterogeneous opposed flow diffusion flame allows interpretation of the limit in solid regression rates in terms of global reaction kinetics. Calculations have been carried out for a range of parameters, including net heats of gasification and activation energies. For the AP-propylene system the experimental data can be fitted to a second-order gas-phase reaction rate with an activation energy of 37 ± 1 kcal/mole and a preexponential coefficient of 10^{13} $cc \cdot mol^{-1}$ sec^{-1}.

I Introduction

An understanding of the solid propellant combustion process is essential for interpretation of motor performance and the prediction of propellant characteristics under various physical conditions. To elucidate the burning mechanism of AP-based composite solid propellant, a number of analyses have been carried out that differ mainly in the degree of complexity of the theoretical models employed.[1*] Common to all these models is the mechanism of (1) conductive heat transport to the propellant surface from the adjoining high-temperature, gaseous reaction zone, (2) gasification of the condensed-phase component (fuel and oxidizer), (3) diffusional mixing of the gaseous constituents, and (4) exothermic chemical reaction in the gas phase. Near the solid/gas interface an AP (ammonium perchlorate) decomposition flame may form part of the reaction zone involving fuel and oxidizer species emanating from the solid propellant in their original chemical composition or modified by intervening chemical process. In addition, subsurface reactions and phase changes of the solid at the surface may make contributions to the regression rate of the solid propellant.

The complex nature of the solid propellant reacting system and the high temperatures involved make the task of elucidating the numerous kinetic steps most formidable. However as a first step in the study of the reaction mechanism it may be adequate to have available information on the "global" reaction kinetics that offer a measure of the heat release rate due to exothermic chemical reaction in the gas phase as a function of temperature, pressure, and gas composition. The availability of such data should permit semiquantitative interpretation of the reaction rates in the flame zone, and provide a better measure of the interplay between diffusional mixing and chemical reaction under various operational conditions.

---

*References are listed after the appendix.

The opposed-jet experimental technique[2] has been used to obtain kinetics parameters in the homogeneous case where jets of gaseous fuel and oxidizer support a diffusion-controlled flame.[3] As the velocity of the jets is increased, a smaller fraction of the incoming reactants are consumed due to kinetic limitations. The unburnt reactants act as diluents carrying away heat from the flame so that at a high enough velocity the flame is extinguished.

The same technique has been applied to the heterogeneous case where a jet of gaseous fuel is directed against a subliming solid oxidizer.[4] As the velocity of the jet is increased, the solid regression rate has been observed to increase to a certain limit, at which a further increase in jet velocity leaves the regression rate unchanged. This limit has been identified to correspond to the maximum fuel consumption rate for the system. At greater flow rates, fuel slips through the flame zone to act as diluent and heat sink near the subliming surface, thus limiting the surface temperature and regression rate. A theoretical model is developed that relates stagnation flow and regression rates to global kinetic parameters and the heat requirement at the subliming surface.

In the following sections we have prepared first a descriptive presentation of the model, the approximations made, and the results obtained. This part is followed by Appendix A containing the details of the mathematical analysis and Appendix B giving the application to the AP-propylene system.

II Theoretical Model

The objective of the theoretical analysis is to relate the rates of chemical reaction occurring in the gas-phase diffusion flame to the combustion characteristics of the heterogeneous opposed-flow diffusion flame (HOFD) set up between a subliming solid oxidizer and a gaseous jet of fuel with inert diluent. Alternatively, the analysis allows deduction of reaction-rate parameters of the gas-phase deflagration from experimental measurements of the HOFD.

The cylindrically symmetric, steady flow field is sketched in Figure 1. It has been assumed that the ratios of jet nozzle radius and distance from the solid to solid stick radius are so large as to be effectively infinite. Although there are two coordinates, radial distance r from the axis of symmetry and axial distance z from the surface of the solid, the flow along the axis is decoupled from the remainder of the flow if one assumes that the radial diffusion of mass and heat is negligible in comparison with axial diffusion and convection. The distributions of temperature and species along the axis are then determined by one-dimensional equations in z only.

The multi-step kinetics of the gas-phase deflagration process are approximated by a global reaction-rate expression. Such an approximation appears to be an adequate quantitative description of the kinetics in terms of local heat-release rates. Obviously it is less satisfactory in terms of an analysis of spatial distribution of chemical intermediates since no detailed account is taken of the mechanism of the reaction and the intermediate species produced.

In Appendix A the conservation equations for mass and energy are formulated in terms of the Shvab-Zeldovitch model with constant, temperature-averaged parameters for the physical and transport parameters, and a Lewis

number of unity. Such a model is based on a single overall reaction involving two gaseous reactants. The coefficients in the equations depend on the axial component of the mass-flux distribution, which in turn is determined by the momentum balance equations. However in the present system the momentum variations are expected to be small so that almost any flow satisfying the mass conservation equation should be an adequate approximation. Spalding[5] and others have assumed, for the case of opposed gaseous jets, a linear variation of the radial velocity component with distance from the axis and a similar variation of the axial component from the plane through the stagnation point and perpendicular to the axis. This flow can be strictly correct only near the stagnation point. Self-similar boundary layer flow has also been employed.[7] This flow has the advantage of providing a solution of the complete set of flow equations. However, it seems inapplicable to the present case where a large regression rate disrupts the boundary layer.

In the present model the axial component of the mass flux is described by a series approximation with a sufficient number of terms to satisfy the conditions at the solid surface and at the inlet for the gaseous reactant. The flow has a stagnation point and exhibits the correct behavior in its neighborhood. The radial component of the flow is determined by the axial mass flux gradient and has in the model the constant sign that implies a realistic radial outflow everywhere. To provide an analytical model for rapid computation and evaluation of different parameters we approximate the temperature distribution by a polynomial in the distance variable. An advantage of the analytic approximation method over asymptotic methods[8] is that no parameter need take extreme values for the approximation to be useful.

In the analysis of HOFD information is needed on the conditions at the gas/solid interface. For the present model, we have employed experimental results[10] relating surface temperature and regression rate.

III Analytical Results

The most striking feature of the experimental results for the AP/fuel system[4] is the observed change from a strong variation of solid regression rate at low values of the fuel mass flux to nearly constant regression rate at higher fluxes. The theoretical model interprets this behavior to be due to a change from complete fuel consumption in one case to unburnt fuel slippage through the flame to the solid surface in the other. In the latter case the unburnt fuel acts as diluent and heat sink.

At very low fuel flow rates the thin-flame approximation applies (Appendix A.9). In this regime the combustion process is controlled by the mass transfer rate of reactants to the flame and is a sensitive function of the heat L of gasification of the solid reactant. The value of L is given by the difference between the heat of sublimation and the exothermic heat of reaction at the solid surface. A series of calculations have been carried out over a range of values of L. The sensitivity of the system to variations in L is exhibited by the data presented in Figures 2 and 3. The lines going through the origin depict the variation of m_S as a function of m_G at different weight fractions of fuel (Y_{FG}) for two values of L. In applying these data to the experimental results obtained for the AP/propylene system[4] one deduces a value of L = 87 ± 1 cal/gm AP (Table 1). It is to be noted that this value is considerably less than the heat of sublimation of AP (450 cal/gm AP), an indication of the contribution of exothermic reactions in the condensed phase. Similar conclusions were drawn in previous studies of the temperature distribution in solid AP during steady-state deflagration[11] and in a modelling analysis of AP combustion.[12]

The kinetic-controlled regime of the HOFD system is demonstrated by the attainment of the solid regression rate limit at high mass fluxes of

gaseous fuel. This condition is represented by the intersection of the straight lines with the curves in the (m_G, m_S) plane of Figures 2 and 3 computed for different values of L and the activation energy E for a single-step reaction of first order in fuel and oxidizer. These data indicate that with increasing E the transition to kinetic control occurs at progressively lower fuel mass fluxes (critical value = m_G^*). However, an increase in the initial fuel concentration (Y_{FG}) exhibits a somewhat more complex pattern. For example the data in Figure 1 indicate that for E = 25 an increase in Y_{FG} from 0.25 to 1.00 causes m_G^* to decrease progressively while m_S^* appears to go through a maximum as observed experimentally.[4] This behavior may be due to the progressive departure from stoichiometric conditions (on the fuel-rich side) as Y_{FG} increases so that the flame cools and the regression rate decreases.

While the computations for Figures 2 and 3 consider all the oxygen in the AP to be available for C_3H_6-oxidation in the flame (Y_{SX} = 0.547), those of Figure 4 consider some of the oxygen consumed for ammonia oxidation (Y_{SX} = 0.400). These computations point to the marked effect of the oxidizer weight fraction at the solid surface on the combustion process. One also notes in Figure 4 that the reduction in the supply of oxidizer has moved the maximum regression rate toward lower values of Y_{FG}, as expected on the basis of a departure from stoichiometry.

The theoretical model is applied to the experimental data[4] for the AP/propylene system. As can be seen the two-regime model represents a satisfactory approximation to the experimental observations (Figure 5). The limiting mass flux m_S^* for each weight fraction of fuel has been recorded in Table 1. This data is used to compute the activation energy E (Appendix A.10). The value for E so obtained should be independent of the fuel weight fraction, as is found to be the case (Table 1). The experimental results yield an activation energy of 37 ± 1 kcal/mole for

the gas-phase reaction associated with the combustion process of AP and propylene.* Thus the rate constant for this reaction may be written as $k = 10^{13} \exp(-37000/RT)$ cc·mol^{-1}sec^{-1}.

IV Conclusions

The opposed flow diffusion flame is a convenient and precise tool for the investigation of kinetic parameters at high temperatures. In the homogeneous case of opposed gaseous jets, the flame is abruptly extinguished on the axis of symmetry when the reactant flow reaches a critical value; extinction occurs when the reactants are no longer completely consumed and therefore act as diluents carrying heat away from the flame. A model of the flow and reaction has been used[3] to derive overall reaction parameters from the opposed flow data.

In the heterogeneous case one stream is produced by gasification of a condensed phase reactant, the other originates as a gas. A model for the HOFD at very low flow rates has been used to relate the ratio of solid and gas mass fluxes to the heat of gasification. Its constancy as the gas composition is varied indicates that a useful explanation of the relation between regression rate and heat of gasification has been found.

Our model further suggests that the levelling-off in observed regression rate curve as the gaseous reactant flow is increased is due to incomplete combustion. These critical conditions can be related to the gas phase reaction rate. The model predicts activation energies that are independent of the gas stream composition. Thus the HOFD offers a unique approach to the evaluation of kinetic parameters of concern to complex combustion systems such as those encountered in solid propellant deflagration.

---

*For $Y_{XS} = 0.400$ one finds a value of $E = 24.5 \pm 2$ kcal/mole AP.

Appendix A

EQUATIONS OF THE MODEL

A.1 Mass and Energy Conservation Equations

For the one-dimensional model employed in our analysis we use the Shvab-Zeldovitch equations[13] which govern mass and energy conservation in convective, diffusive, reactive, steady-state flow. To reduce the degree of complexity of the problem without materially affecting the validity of the model the simplifying assumptions are made that the binary diffusion coefficient D is the same for all species and the Lewis number is unity, so that heat conductivity λ is related to the gas density ρ and average specific heat $\bar{C}_p$ by $\lambda = \rho D \bar{C}_p$. We may write therefore:

$$\nabla \cdot (\rho \bar{v} Y_i - \rho D \nabla Y_i) = w_i$$

$$\nabla \cdot (\rho \bar{v} \bar{C}_p T - \rho D \bar{C}_p \nabla T) = -\Sigma h_i^o w_i ,$$

where $\bar{v}$ is the velocity vector, w_i is the rate of formation of species i in the single step reaction, Y_i is the mass fraction and h_i^o the heat of formation of the species, and T is the temperature. If C_{pi} is the specific heat at constant pressure of species i then $\bar{C}_p$ is defined by

$$\bar{C}_p T = \Sigma_i Y_i \int_o^T C_{pi} \, dT ,$$

The stoichiometry of the reaction may be expressed as:

$$\Sigma \nu_i' M_i \rightarrow \Sigma \nu_i'' M_i ,$$

where M_i is the chemical symbol for species i and the ν_i' and ν_i'' are stoichiometric ratios. Then

$$w_i = W_i (\nu_i'' - \nu_i') \omega ,$$

where W_i is the molecular weight of species i and molar reaction rate ω is independent of i. The mole fraction of species i is X_i :

$$X_i = (Y_i/W_i)/\Sigma\,(Y_k/W_k) .$$

Define the heat of reaction Q by

$$Q = -\Sigma\, h_i^o\, W_i\, (\nu''_i - \nu'_i)/W_o ,$$

where W_o is a constant molecular weight. Then the conservation equations read

$$L(\alpha_i) = L(\alpha_T) = \omega W_o ,$$

where

$$\alpha_i = Y_i W_o/W_i\, (\nu''_i - \nu'_i)$$

$$\alpha_T = \bar{C}_p T/Q ,$$

and differential operator L is defined by

$$L(\alpha) = \rho v\cdot\nabla \alpha - \nabla\cdot\rho D\nabla\alpha .$$

The equation for conservation of total mass ,

$$\nabla\cdot(\rho\bar{v}) = 0 ,$$

has been used to simplify L .

A.2 Axis Approximation

On the axis of cylindrical symmetry vector $\bar{v}$ has just the one component v in the z-direction so that

$$L(\alpha) = \rho v \frac{\partial\alpha}{\partial z} - \nabla\cdot\rho D\nabla\alpha .$$

Neglecting radial diffusion gives the one-dimensional equation

$$L(\alpha) = \rho v \frac{d\alpha}{dz} - \frac{d}{dz} \rho D \frac{d\alpha}{dz} .$$

The equation has a simpler form if the axial coordinate is changed from z to the dimensionless coordinate y :

$$y = m_o \int_o^z (1/\rho D)\, dz ,$$

where m_o is a constant mass flux. Then

$$L(\alpha) = \frac{m_o^2}{\rho D} \left(\frac{\rho v}{m_o} \frac{d\alpha}{dy} - \frac{d^2\alpha}{dy^2} \right).$$

For definiteness m_o is taken to be m_G, the mass flux at the gas inlet,

$$m_G = -\rho v \text{ at } z = \infty .$$

and the origin of coordinates, z=0, is put at the surface of the solid.

A.3 Flow Field

If s stands for any of the differences $(\alpha_i - \alpha_T)$ or $(\alpha_i - \alpha_j)$ then

$$L(s) = 0$$

or

$$ms' - s'' = 0, \; m = \rho v / m_G ,$$

where the prime denotes differentiation with respect to y . This can be solved for a non-constant solution function s if m is given as a function of y . Conversely if s is given, m is determined.

In order that s may replace y as a coordinate, one requires $s' \neq 0$. Also, for convenience,

$$s = 0 \quad \text{at} \quad y = 0 \,,$$

$$s = 1 \quad \text{at} \quad y = \infty \,,$$

so that s' is positive. Conditions on m are

$$m = m_S/m_G \quad \text{at} \quad y = 0$$

$$m = -1 \quad \text{at} \quad y = \infty$$

where m_S is the mass flux at the surface of the solid. The y coordinate of the stagnation point, y_o, is found by solving

$$m = 0 \text{ at } y = y_o .$$

In the experiment, there is a cylindrical nozzle for the gas inlet and the oxidizer has the shape of a solid cylinder. The ratios of solid diameter to nozzle diameter and distance to the nozzle are parameters controlling the flow configuration, in general. However, both ratios were taken sufficiently large in the experiments so that no effect of further variations was observed. Thus both ratios are essentially infinite, and the geometrical configuration does not enter the calculations explicitly.

In order that m = -1 at $y = \infty$, function s' should be proportional to exp(-y) when y is large. A function of this sort is

$$s = 1 - \exp(-y - f)$$

with f bounded at infinity. A convenient choice is to make f a polynomial in [y/(y + b)] where b is a constant taken to be positive so that the flow region is free of singularities. One finds

$$s' = (1 - s)(1 + f')$$

$$m = f''/(1 + f') \cdot (1 + f')$$

$$m' = f'''/(1 + f') - [f''/(1 + f')]^2 - f''$$

Conditions at infinity have been satisfied. We take f to be quadratic:

$$f = a_o + a_1 x + a_2 x^2 , \qquad x = y/(y + b) .$$

Differentiation gives

$$f' = [(1 - x)^2/b] (a_1 + 2a_2 x) ,$$

$$f'' = [2 (1 - x)^3/b^2] (a_2 - a_1 - 3a_2 x) ,$$

$$f''' = [6 (1 - x)^4/b^3] (a_1 - 2a_2 + 4a_2 x) .$$

The conditions at y = 0 give

$$a_o = 0 ,$$

$$a_2 = a_1 + (a_1 + b)(a_1 + Mb)/2 , \quad M = 1 + m_S/m_G ,$$

$$s_o' = 1 + a_1/b ,$$

$$m_S' = 2 [3(b + a_1)(a_1 - 2a_2) - 2 (a_2 - a_1)^2 - (b + a_1)^2 (a_2 - a_1)]/b^2 (b + a_1)^2 ,$$

where s_o' is the value of s' at s = 0 and m_S' is the value of m' there.

The requirements that b and s_o' be positive restrict the choice of a_1 and a_2 to the region $-b < a_1 < a_2$. In addition, a physically reasonable flow has m' negative throughout. Ensuring this in general seems difficult; however, if one takes $a_2 = -(1/2)a_1$ and restricts

a_1 to $-b < a_1 < 0$, then the formulas simplify and one can readily see that this condition is satisfied.

The simplified formulas obtained when $a_2 = -(1/2)a_1$ read

$$f = a_1 x (1 - x/2) ,$$

$$f' = (a_1/b)(1 - x)^3 ,$$

$$f'' = -3(a_1/b^2)(1 - x)^4 ,$$

$$f''' = 12(a_1/b^3)(1 - x)^5 .$$

A.4 Boundary Conditions

If T_S is the surface temperature of the solid and T_A the ambient temperature, the heat flux into an inert solid in the steady state is

$$\lambda_S \frac{dT}{dz} = m_S C_S (T_S - T_A) ,$$

where λ_S is the conductivity and C_S is the specific heat of the solid. Equations for the conservation of heat and species across the surface read

$$\lambda \frac{dT}{dz} = m_S L + \lambda_S \frac{dT}{dz}\Big|_S$$

$$-\rho D \frac{dY_i}{dz} = m_S (Y_{Si} - Y_i) ,$$

where L is the net heat of gasification of the solid and Y_{Si} is the mass fraction of species i in the vapor given off by the solid.

Define α_{Si} to conform to α_i :

$$\alpha_{Ci} = Y_{Si} W_o / W_i (\nu_i'' - \nu_i') .$$

Then the species boundary condition becomes

$$m_G \alpha_i' = m_S (\alpha_i - \alpha_{Si}) \quad \text{at} \quad y = 0 .$$

The heat condition for the inert solid reads

$$\alpha_T' = (m_S/m_G) [(L/Q) + (C_S/\bar{C}_p) (\alpha_{TS} - \alpha_{TA})] \quad \text{at } y = 0 ,$$

where the variation of $\bar{C}_p$ with temperature and concentration ratios has been neglected. If there is heat release by reaction in the solid phase, the heat condition has a different form. Only inert solid is treated here.

At the gas inlet, the temperature and species concentrations have known values:

$$\alpha_T = \alpha_{TG} , \alpha_i = \alpha_{iG} , \text{ at } s = 1 .$$

A.5 Species Distributions

The distribution of species i is related to that for temperature by

$$\alpha_i = \alpha_T - A_i - B_i s ,$$

where A_i and B_i are constants determined by the boundary conditions. One finds

$$A_i = \alpha_{TS} - \alpha_{iS} ,$$

$$A_i + B_i = \alpha_{TG} - \alpha_{iG} ,$$

$$s_o' B_i = (m_S/m_G) [(L/Q) + (C_S/\bar{C}_p) (\alpha_{TS} - \alpha_{TA}) - (\alpha_{iS} - \alpha_{Si})] .$$

These conditions are used to determine A_i, B_i, and α_{iS} for given s_o', M, and α_{TS} .

A.6 Reaction Rate Equation

The Arrhenius gas phase reaction rate expression may be written as

$$\omega = BT^{n} e^{-E/R_o T} \Pi (X_j \rho/R_o T)^{n_j} ,$$

where E is the activation energy, R_o the gas constant, B and n are constants, n_j is the order of the reaction with respect to reactant j, and index j ranges over the species consumed in the reaction. Here j = F or X .

Let $\bar{W}$ be the average molecular weight,

$$\bar{W} = 1/\Sigma(Y_i/W_i) .$$

Then $X_j = Y_j \bar{W}/W_j$ so that the X_j can be eliminated. Neglecting the variation in $\bar{W}$ allows one to set $W_o = \bar{W}$. Since Y_j and T are proportional to the variables of the theory, α_j and α_T, one obtains

$$\omega = B (p/R_o)^{\Sigma n_j} (Q\alpha_T/\bar{C}_p)^{n-\Sigma n_j} e^{-E'/\alpha_T} \Pi (-\nu_j' \alpha_j)^{n_j} ,$$

$$E' = E \bar{C}_p/R_o Q .$$

The equation for conservation of energy,

$$L (\alpha_T) = \omega \bar{W} ,$$

simplifies when the independent variable y is replaced by s to read

$$\alpha_T'' + R = 0 , \quad R = (\omega \bar{W}) [\rho D/m_G^2 (s')^2] ,$$

where the dots indicate differentiation with respect to s.

The dependence of ρD on the temperature is given by

$$\rho D = \rho_A D_A (T/T_A)^{d} .$$

Then

$$R = B'(s')^{-2}\, \alpha_T^{n+d-\Sigma n_j}\, e^{-\mathcal{E}'/\alpha_T} \prod (A_j + B_j s \cdot \alpha_T)^{n_j} ,$$

$$B' = (\bar{B}\bar{W}/m_G^2)\, \rho_A D_A T_A^{-d}\, (p/R_o)^{\Sigma n_i}\, (Q/\bar{C}_p)^{n+d-\Sigma n_j} \prod (\nu_j')^{n_j} .$$

Boundary conditions on α_T read

$$\alpha_T = \alpha_{TG} \quad \text{at } s = 1 ,$$

$$s_o' \alpha_T^{\bullet} = (m_S/m_G)\, [(L/Q) + (C_S/\bar{C}_p)\, (\alpha_T - \alpha_{TA})] \text{ at } s = 0 .$$

The curve in the (s, α_T) plane representing the solution lies inside the polygon defined by

$$0 \le s \le 1 , \quad 0 \le \alpha_T , \quad \alpha_T \le A_j + B_j s .$$

The function R is positive inside the polygon and is zero on the sides, except the sides s = 0 and s = 1. The differential equation shows that the second derivative or, for brevity, "curvature" of the solution curve is equal to (-R). Where reaction occurs, rate function R is positive and the solution curve is convex above, i.e., arched.

A.7 Approximate Temperature Distribution

Possible solution curves for dimensionless temperature α_T as a function of distorted distance coordinate s are sketched in Figure 6. Point A represents the thin, diffusion-controlled flame for which the reaction rate is so fast relative to the rates for diffusion and convection that both reactants are completely consumed at the flame surface. For this case, reaction rate function R is infinitely large in the interior of the polygon, but is zero on its sides.

For finite, decreasing values of R the reaction zone broadens, and temperature curves are found like those labelled 1 to 4 in Figure 6. Point V, where R is a maximum, has been taken in the model as the flame location. It should be close to the points of maximum temperature and maximum reaction rate.

The temperature distribution is approximated in the model by a polynomial in s that fits the energy conservation equation at three points, the two edges of the flame zone and a point V at the "center" of the flame where the reaction rate is a maximum. A polynomial of fourth degree is required to fit the second order equation and its two boundary conditions:

$$\alpha_T = b_o + b_1 s + b_2 s^2 + b_3 s^3 + b_4 s^4 .$$

At Point V, we have

$$\alpha_{TV} = \sum_{j=o}^{4} b_j s_V^j$$

$$\Sigma\, j(j-1)\, b_j s_V^{j-2} + R_V = 0$$

$$R_{,sV} + R_{,\alpha_T V} \Sigma\, j\, b_j s_V^{j-1} = 0$$

where, in the last equation, the subscript commas indicate partial differentiation. From the formula for reaction rate function R one finds

$$R_{,s} = (-2m + n_F B_F/Z_F + n_X B_X/Z_X)\, R ,$$

$$R_{,\alpha_T} = [E'/\alpha_T^2 + (n + d - n_F - n_X)/\alpha_T - n_F/Z_F - n_X/Z_X]\, R ,$$

$$Z_F = A_F + B_F s - \alpha_T , \quad Z_X = A_X + B_X s - \alpha_T .$$

The remaining equations and boundary conditions needed to determine the b_j depend on which type of solution curve is applicable. If both fuel and oxidizer are completely consumed, the curve will be like Type 1 as sketched in Figure 6. In the limit where the fuel is just consumed before reaching the solid surface, the curve is of Type 2. The equations that follow are written for Type 1 and apply to its limit, Type 2. The other types, with incompletely consumed fuel, were not used in the comparisons with the experimental observations.

If point (s_X, α_{TX}) is at the inlet edge of the reaction zone,

$$\alpha_{TX} = \Sigma\, b_j\, s_X^j$$

$$\alpha_{TX} = A_X + B_X s_X$$

$$\Sigma\, j\, b_j\, s_X^{j-1} = B_X$$

$$\Sigma\, j\,(j-1)\, b_j\, s_X^{j-2} = 0 ,$$

where the model polynomial passes through the point according to the first equation, the point lies on $Y_X = 0$ according to the second equation, in the third equation the curve is given the slope of $Y_X = 0$ since slope is proportional to heat flux and is therefore continuous, and in the

fourth equation the curve is given zero second derivative as determined by the differential equation being fitted. At the other edge of the reaction zone the same equations are valid if subscript X is replaced with F.

The 11 equations above may be solved for the 11 unknowns: the 5 b_j's and the pairs of coordinates of Points V, F, and X.

A.8 The Solid-Gas Interface

In an experiment with a known reactive system the material, kinetic, and configuration parameters would be known. If conditions permitted a steady-state flame, values for the surface temperature, flame location, and regression rate could be measured. A complete model therefore requires that these quantities be computable. It has been shown above that the regression rate is determined in the model if the surface temperature and parameter s_o' are given.

Since the details of the gasification process at the solid surface are not known in quantitative detail, the model has been completed by using the empirical relation[10] between surface temperature T_S(°K) and regression rate:

$$m_S = 1.8 \exp (14.9 - 16500/T_s) \text{ (gm/cm}^2\text{-sec)}.$$

Specification of s_o' has been achieved at two limiting points by use of the extra conditions valid there. The thin-flame limit is discussed in the next section. The other limit is where the reaction zone just reaches the surface of the solid. The extra condition, $s_F = 0$, is an indirect specification of the free parameter. This limit gives a change of flame character in the model and is taken to coincide with the observed changes in rate of change of regression rate with inlet flow shown in Figure 5.

A.9 Low-Flow Regime

If the inlet gas mass flux m_G is small, a steady flow solution has very low reaction rate ω almost everywhere since the reaction rate function R is proportional to $\omega(m_G s')^{-2}$ and R and s' are bounded. This condition is the thin-flame approximation without any fuel on one side of the flame or any oxidizer on the other. In particular, at the surface of the solid, the slope of the solution curve α'_{TS} is related to the other parameters B_F and s'_o by

$$s'_o = \alpha'_{TS} / B_F .$$

The pressure variation due to flow acceleration is

$$-p_z = \rho v v_z = m_G^3 (R_o Q/\rho_A D_A \bar{C}_p) m(m\alpha_T)' .$$

Thus p_z goes to zero with m_G^3 due to dimensional considerations. It seems reasonable that the nondimensional flow pattern also contributes to the smoothing out of the pressure variations. It is therefore assumed that $(m\alpha_T)'$ also goes to zero with m_G at the surface of the solid. This gives

$$m'_S \alpha_{TS} + (m_S/m_G) \alpha'_{TS} = 0 .$$

The flow model provides an expression for m'_S in terms of s'_o and (m_S/m_G):

$$m'_S = - (s'_o + M-1) [3M - 3 + (M + 5) s'_o - 2(s'_o)^2]/3(1 - s'_o) ,$$

where $M = (m_S/m_G) + 1$. One may then solve for the value of (m_S/m_G) in the low-flow limit:

$$m_S/m_G = 3\,[\beta - \alpha\,(1+\beta)(1+2\beta)]/\beta\,[3\beta + \alpha\,(1+\beta)(1-2\beta)]$$

where

$$\alpha = \alpha_{TS}/B_F \quad ,$$

$$B_F = \alpha_{TG} - \alpha_{FG} - \alpha_{TS} \quad ,$$

$$\beta = [L/Q + (C_S/\bar{C}_p)(\alpha_{TS} - \alpha_{TA})]/B_F \quad ,$$

and, if $T_G = T_A$, $\alpha_{TS} = \alpha_{TA}$. If $\alpha \ll 1$ the relation simplifies to

$$\beta = \alpha + \gamma^2\,(9 + 4\,m_S/m_G)/3 \quad .$$

A.10 Calculation Method

For a specified reaction system the calculation requires knowledge of the species present, the reaction stoichiometry, the ambient and inlet temperatures, the weight fraction Y_{FG} of fuel in the inlet stream and the weight fraction Y_{SX} of oxidizer in the solid. Values for the specific heats, C_s and $\bar{C}_p$, and the heat of combustion Q are also known so that the nondimensional quantities α_{TA}, α_{TG}, α_{FG} are determined. In the low flow limit (Section A.9), if $T_A = T_G$, one has $\alpha_{TS} = \alpha_{TA}$ so that B_F is known and the relation between heat of gasification L and low-flow mass-flux ratio m_S/m_G is fixed. The observed value of this ratio determines L.

For the case of complete combustion of the gaseous fuel and no fuel in the solid, one has $Y_{FS} = Y_{SF} = 0$. The mass-flux ratio m_S/m_G is assumed to remain constant up to the limit of complete combustion. For each m_S, the empirical regression relation[10] determines the surface temperature T_S. The values of A_F, and B_F, and s_o' are then computable

from the boundary conditions for the fuel species at the solid surface given in Section A.5. The three oxidizer boundary conditions then serve to compute A_X, B_X, and α_{XS} or Y_{XS}, the mass fraction of oxidizer in the gas at the solid surface.

For specified kinetic parameters, the reaction rate function R is now a computable function of s and α_T. The conditions on the temperature distribution parameters given in Section A.7 can be readily reduced to a pair of nonlinear equations for s_F and s_X, the s coordinates of the edges of the reaction zone. (At s_F the fuel concentration drops to zero; while at s_X the oxidizer concentration drops to zero.) The equations have been solved for s_F and s_X by a two-variable version of Newton's method.

The computations were carried out for different values of the regression rate m_S. As the limiting solution that value of m_S was selected for which the reaction zone extended to the solid surface so that $s_F = 0$.

Appendix B

APPLICATION OF THEORETICAL ANALYSIS TO THE AP-FUEL SYSTEM

To demonstrate the suitability of the theoretical model for evaluation of reaction kinetics of a heterogeneous combustion system we have carried out a series of calculations for the opposed-flow diffusion flame of solid AP-gaseous propylene, for which experimental data are available.[4] The reaction is considered to involve the thermal decomposition of AP during the gasification process with subsequent combustion between the oxygen produced and the propylene added in accordance with the stoichiometry

$$C_3H_6 + 1/2\ O_2 \rightarrow 3\ CO_2 + 3\ H_2O$$

In the current analysis the contribution of fuel from the subliming solid (AP) is taken to be small compared to that introduced from the gaseous fuel side (C_3H_6). Consequently we do not consider explicitly the formation of a premixed flame in close proximity of the solid surface due to the reaction of the decomposition products of AP (NH_3 and $HClO_6$, or its oxidizer intermediates) as postulated in the granular diffusion flame model.[14] Such exothermic reactions are buried in the gasification term used in our analysis and together with solid-phase exothermic reactions contribute to a reduction in the absolute value of the heat of sublimation of AP from 480 cal/g AP[15] to 87 cal/g AP. However, in order to examine the effect of oxygen concentration Y_{SX} at the solid surface on the reaction kinetics of the diffusion flame we have carried out several computer calculations at two levels of Y_{SX}, one for $Y_{SX} = 0.547$ corresponding to all the oxygen in solid AP, the other at $Y_{SX} = 0.4$ corresponding to some oxygen depletion (due to reaction with ammonia). For the conditions prevailing at the gaseous fuel side we have selected three fuel weight fractions, i.e., 0.32, 0.60, and 1.00 corresponding

to 24, 50, and 100 vol% of propylene, as employed during the experimental study. The remaining input parameters for the computer calculations are listed in Table 2.

A comparison of the present two-regime model with the experimental data[4] is made in Figure 5. The model is fitted to the data at the two extremes of m_s near zero and m_s at its limiting value m_s^*.

REFERENCES

1. Reviews are to be found in J. A. Steinz, P. L. Stang, and M. Summerfield, AIAA Publication 65-658, and J. S. Ebenezer, R. B. Cole, and R. I. McAlevy, III, Technical Report ME-RT 73004, Stevens Inst. Technology, Hoboken, N. J., June, 1973.

2. A. E. Potter and J. N. Butler, Amer. Rocket Soc. J., 29, 54 (1959).

3. C. M. Ablow and H. Wise, Combustion and Flame, 22, 23 (1974).

4. S. J. Wiersma and H. Wise, "Solid Propellant Kinetics. IV. Measurement of Kinetic Parameters in Opposed Flow Solid Propellant Diffusion Flames," Interim Technical Report, Contract N00014-70-C-0155, Office of Naval Research, Power Branch (December 1973).

5. D. B. Spalding, Amer. Rocket Soc. J., 31, 763 (1961).

6. F. E. Fendell, J. Fluid Mech., 21, 281 (1965).

7. L. Krishnamurthy and F. A. Williams, "A Flame Sheet in the Stagnation-Point Boundary Layer of A Condensed Fuel," paper presented to Western States Section, The Combustion Institute, Tempe, Arizona, April 1973.

8. A. Liñán, "Asymptotic Structure of Counterflow Diffusion Flames for Large Activation Energies," Instituto Nacional de Técnica Aeroespecial, Madrid (1973) unpublished.

9. C. Guirao and F. A. Williams, "Models for the Sublimation of Ammonium Perchlorate", Paper 69-22, Western States Section, The Combustion Institute, China Lake, April 1969.

10. J. F. Lieberherr, 12th Symposium (International) on Combustion (1968), 533-541.

11. H. Wise, S. H. Inami, and L. McCulley, Combustion and Flame 11, 483 (1967).

12. C. Guirao and F. A. Williams, "A Model for Ammonium Perchlorate Deflagration between 20 and 100 atm," AIAA J. Vol. 9, pp. 1345-1356 (1971).

13. F. A. Williams, Combustion Theory, (Addison-Wesley, Palo Alto, 1965).

14. M. Summerfield, G. S. Sutherland, M. J. Webb, H. J. Taback, C. P. Hall, "Burning Mechanism of Ammonium Perchlorate Propellants", in Solid Propellant Rocket Research, M. Summerfield, ed.,(Acad. Press, N.Y. 1960).

15. S. H. Inami, W. A. Rosser, and H. Wise, Combustion and Flame, 12, 41 (1968).

Table 1

COMPARISON OF THEORETICAL AND EXPERIMENTAL DATA FOR THE DOFD SYSTEM: AMMONIUM PERCHLORATE-PROPYLENE

Inlet Fuel Mass Fraction Y_{FG}	Initial Mass Flux Ratio $(m_S/m_G)_i$		Final Regression Rate $m_S^* \times 10^2$ (gm/cm^2-sec)	Activation Energy E (kcal/mol)	
	Experiment[4]	Theory[a]	Experiment[4]	Theory[ab]	Theory[ac]
0.32	2.4	2.59	3.10	36.9	26.5
0.60	5.3	6.65	3.96	36.0	23.4
1.00	10.0	12.4	3.75	37.6	23.5

[a] Computed using L = 87 (cal/gm AP)

[b] Computed using $Y_{SX} = 0.547$

[c] Computed using $Y_{SX} = 0.4$

Table 2

INPUT PARAMETERS

Quantity	Symbol	Value
Molecular weight-fuel	W_F	42 gm/mol
-oxidizer	W_X	32 gm/mol
Pressure (1 atm)	p	0.0242 cal/cc
Gas conductivity at ambient conditions	λ_A	6.0×10^{-5} cal/cm-sec-°K
Gas density at ambient conditions	ρ_A	1.25×10^{-3} gm/cc
Lewis number	$\lambda_A/\rho_A D_A \bar{C}_p$	1
Ambient temperature	T_A	300 °K
Inlet temperature	T_G	300 °K
Solid density	ρ_S	1.8 gm/cc
Temperature dependence		
of ρD	d	0
of B	n	0
Order of reaction		
for fuel	n_F	1
for oxidizer	n_X	1
Stoichiometric coefficient		
for fuel	ν'_F	1
for oxidizer	ν'_X	4.5
Specific heat - solid	C_S	0.25 cal/°K
- gas	$\bar{C}_p$	0.25
Arrhenius preexponential	B	10^{13} cc·mol^{-1}sec^{-1}

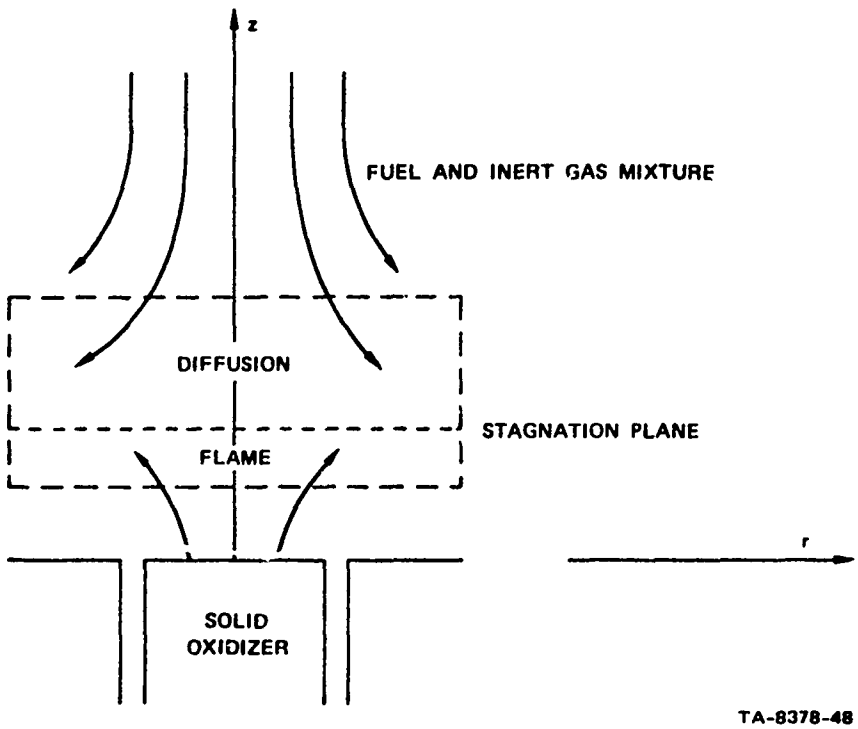

FIGURE 1 SCHEMATIC CROSS-SECTION OF HOFD FLAME

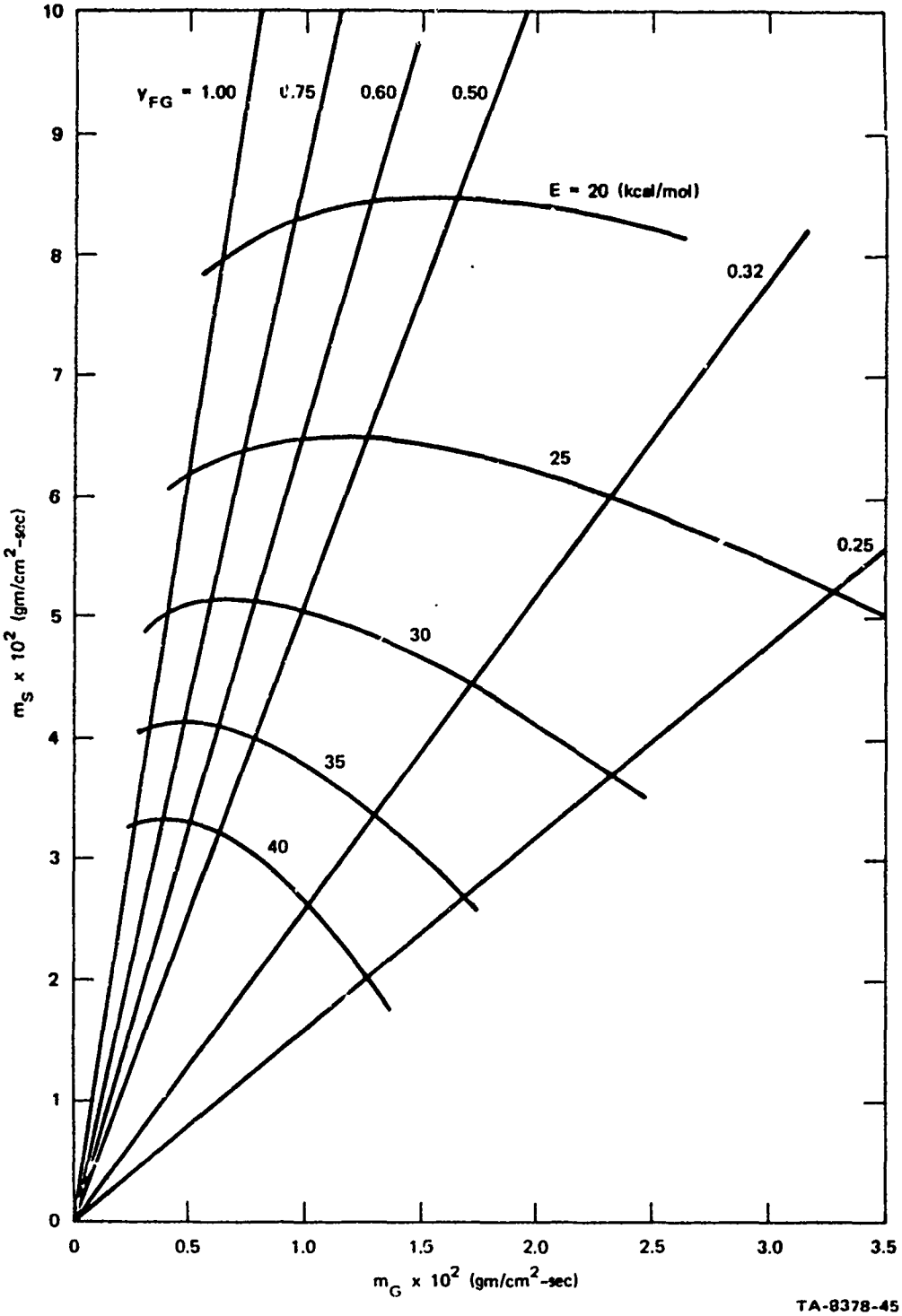

FIGURE 2 THEORETICAL REGRESSION RATE m_S VERSUS INLET FLOW m_G LINES AND COMPLETE COMBUSTION LIMIT CURVES (Y_{XS} = 0.547, L = 87 cal/gmAP)

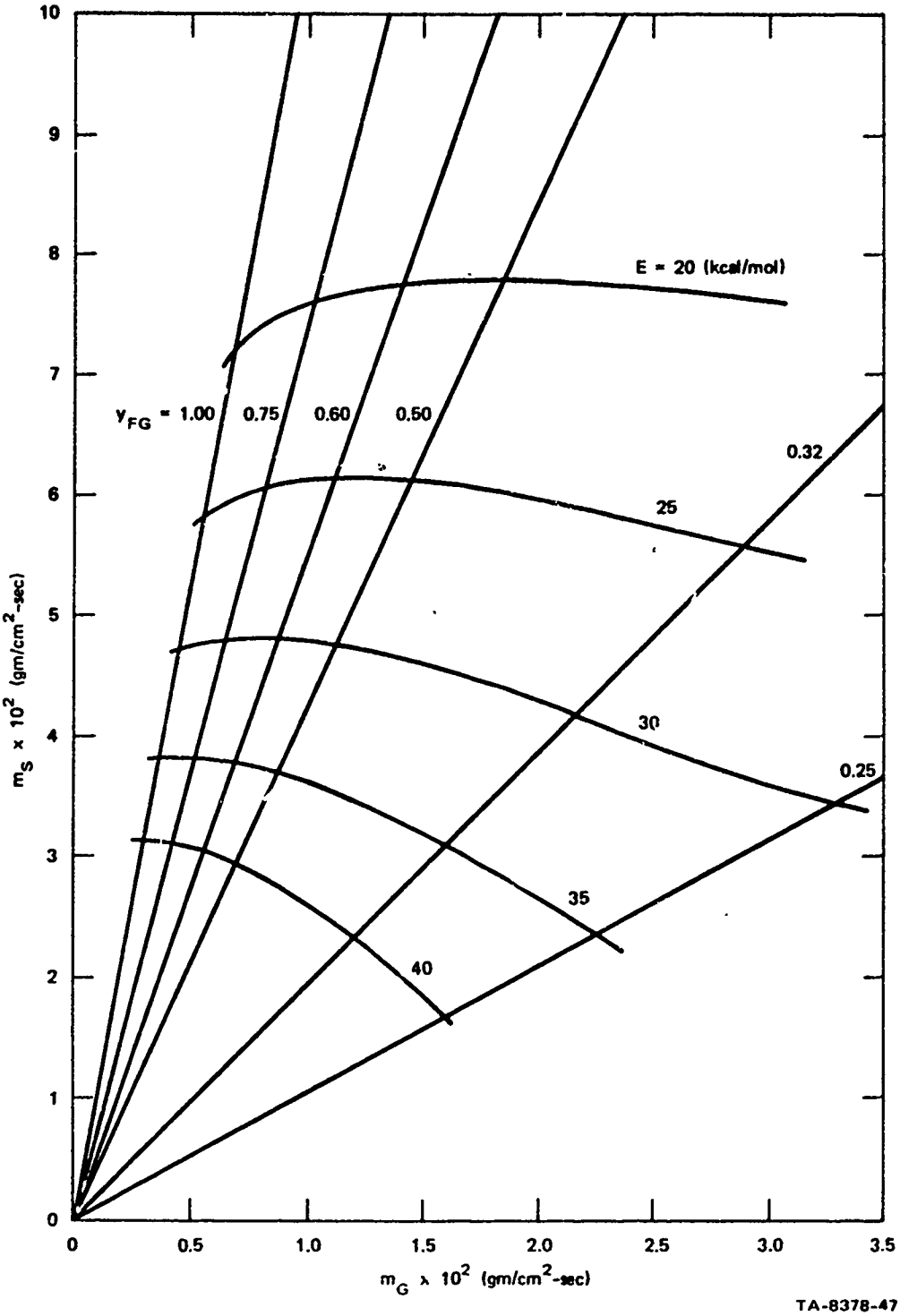

FIGURE 3 THEORETICAL REGRESSION RATE m_S VERSUS INLET FLOW m_G LINES AND COMPLETE COMBUSTION LIMIT CURVES (Y_{XS} = 0.547, L = 85 cal/gmAP)

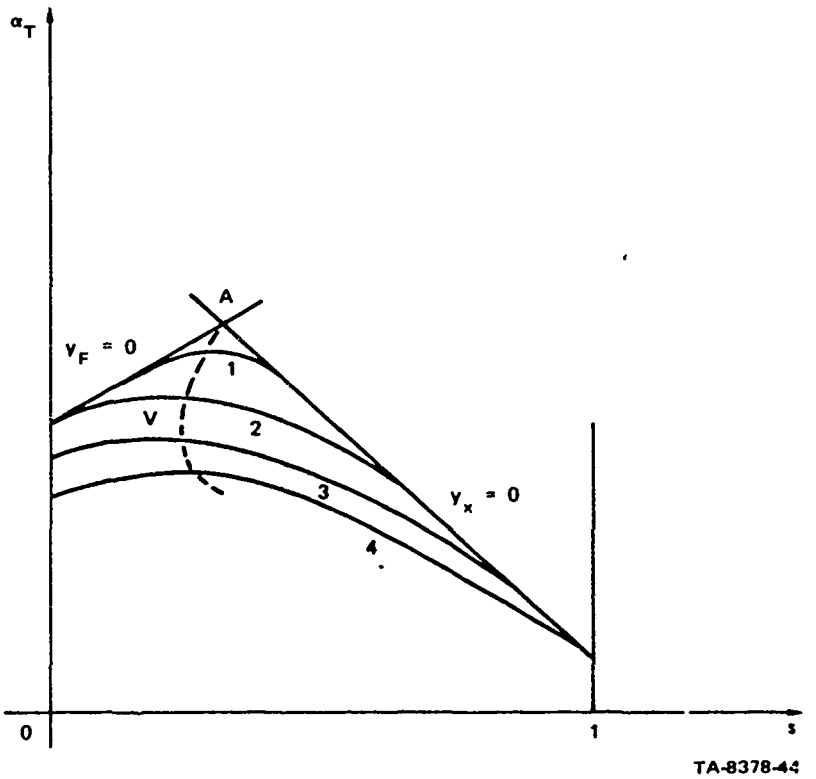

FIGURE 6 NONDIMENSIONAL TEMPERATURE α_T AS A FUNCTION OF DISTORTED DISTANCE s

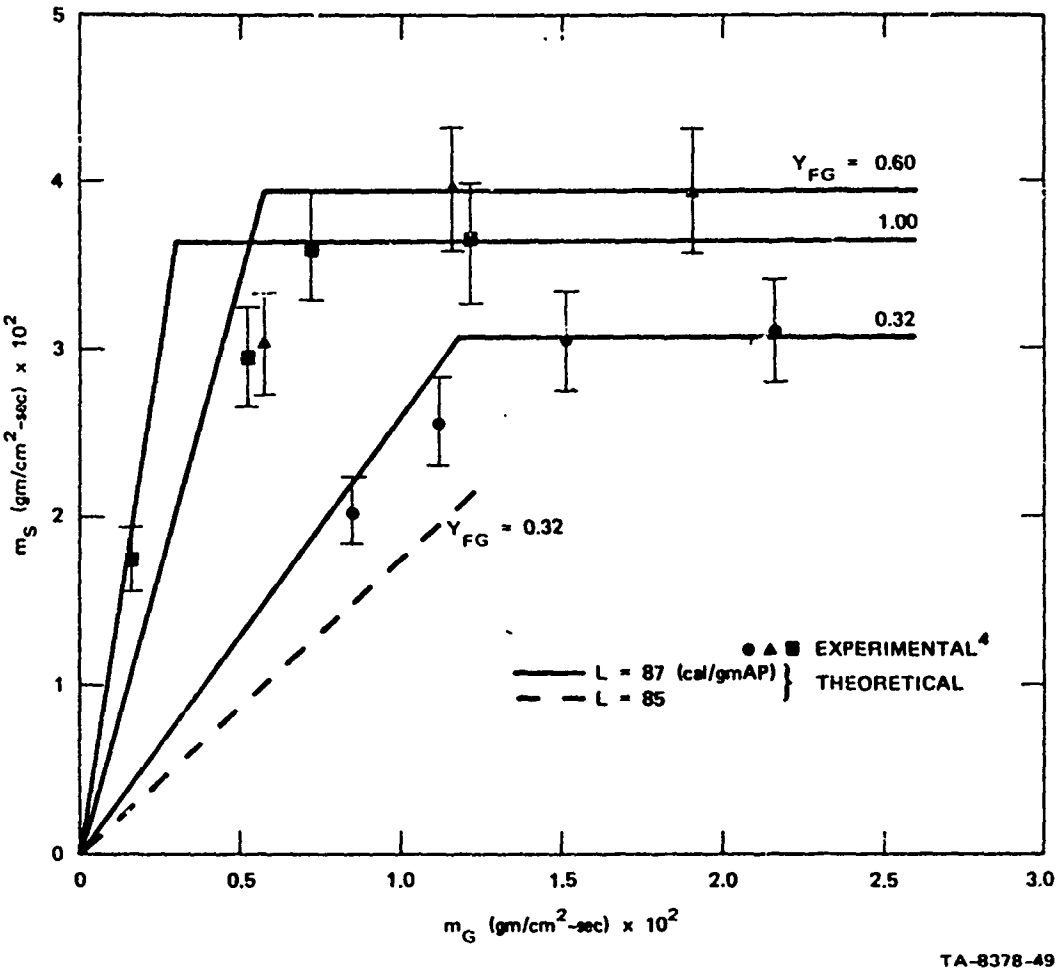

FIGURE 5 HOFD BURNING CHARACTERISTICS FOR THE AP/PROPYLENE SYSTEM

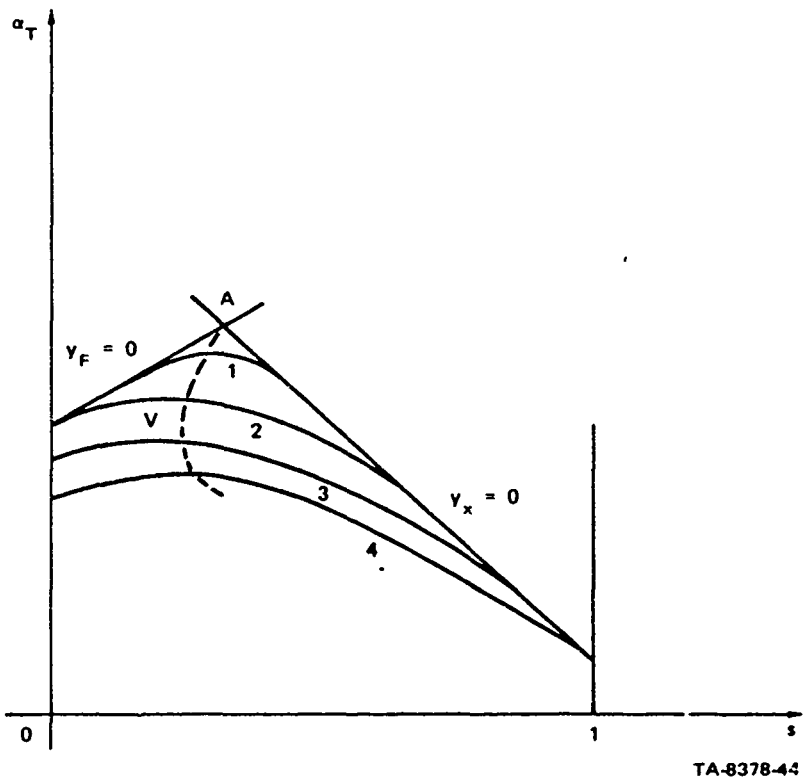

FIGURE 6 NONDIMENSIONAL TEMPERATURE α_T AS A FUNCTION OF DISTORTED DISTANCE s